JPET Fast Forward. Published on July 6, 2011 as DOI: 10.1124/jpet.111.182055

Title page

Role of Vimentin in the Inhibitory Effects of Low-Molecular-Weight Heparin on PC-3M Cell Adhesion to, and Migration through, Endothelium

Yan Pan, Tianluo Lei, Bao Teng, Jihong Liu, Jianzhao Zhang, Yu An, Yuan Xiao, Jing Han, Xueyang Pan, Junhua Wang, Heming Yu, Hong Ren, Xuejun Li

State Key Laboratory of Natural and Biomimetic Drugs, Department of Pharmacology, School of Basic Medical Sciences, Peking University and Institute of System Biomedicine, Peking University, Beijing 100191, China;

Running title: Regulation of vimentin by LMWH inhibits cell migration**.**

Address correspondence to:

Xuejun Li, Department of Pharmacology, School of Basic Medical Sciences, Peking University, Beijing 100191, China; Tel and Fax:82802863; E-mail: xjli@bjmu.edu.cn

Number of text pages (35)

Number of tables (0)

Number of figures (10)

Number of references (40)

Abstract (220 words)

Introduction (354 words)

Discussion (1232 words)

Abbreviations

BSA: bovine serum albumin

CFDA: carboxyfluorescein diacetate

DMSO: dimethyl sulfoxide

DTT: dithiothreitol

EC: endothelial cell

ECL: enhanced chemiluminescence

EDC: *N*-ethyl-*N*'-(3-dimethylaminopropyl)carbodiimide

JPET Fast Forward. Published on July 6, 2011 as DOI: 10.1124/jpet.111.182055
This article has not been copyedited and formatted. The final version may differ from this version.

EDTA: ethylenediaminetetraacetic acid

FBS: fetal bovine serum

HUVEC: human umbilical vein endothelial cell

IEF: isoelectric focusing

IP: inositol phosphate

IPG: immobilized pH gradient

LMWH: low-molecular-weight heparin

MALDI-TOF-MS: matrix-assisted laser desorption ionization time-of-flight mass spectrometry

MMP: matrix metalloprotease

NF-κB: nuclear factor kappa B

NHS: *N*-hydroxysuccinimide

PBS: phosphate-buffered saline

pI: protein isoelectric point

PI: propidium iodide

PMSF: phenylmethylsulfonyl fluoride

RU: response units

SDS-PAGE: sodium dodecyl sulphate–polyacrylamide gel electrophoresis

SEM: scanning electron microscopy

SPR: surface plasmon resonance

TGF-β: transforming growth factor-beta

VEGF: vascular endothelial growth factor

JPET Fast Forward. Published on July 6, 2011 as DOI: 10.1124/jpet.111.182055
This article has not been copyedited and formatted. The final version may differ from this version.

ABSTRACT

Low-molecular-weight heparin (LMWH) has been used in cancer patients with venous thromboembolic complications, resulting in a higher survival rate and an inhibitory action on experimental metastasis. In the present study, human umbilical vein endothelial cells (HUVECs) were treated with LMWH for 24 h, and found that the resulting HUVECs could significantly inhibit the highly metastatic human prostate cancer cell line (PC-3M) in terms of its adhesion to the endothelium and migration across the endothelium, according to scanning electron microscopy. We also determined the elevated levels of endothelial intercellular Ca^{2+} concentration after the adhesion of PC-3M cells to HUVECs was greatly reduced by incubation with LMWH. Using proteomics, we surveyed the global protein changes in HUVECs after LMWH treatment and identified four downregulated proteins that were possible isoforms of cytoskeletal vimentin intermediate filaments, cartilage-derived C-type lectin, and serine/threonine protein phosphatase PP1-beta (PP-1B). LMWH affected the morphology of vimentin and the expression levels of α_v integrin and PP-1B in HUVECs bound to PC-3M cells. Vimentin assists in the adhesion of PC-3M cells, which was confirmed by siRNA experiments. Furthermore, the direct binding of purified vimentin protein with LMWH was detected with surface plasmon resonance (SPR) methods. However, when we used fluorescence-labeled heparin for 24 h to identify whether this binding occurred within cells, heparin was principally distributed around endothelial cells. Taken together, these findings suggest that the mono-incubation of LMWH with HUVECs could inhibit PC-3M cell adhesion to, and

migration through, endothelium; LMWH's regulation of vimentin plays a role in the anti-metastatic action.

Introduction

Metastasis is the main obstacle in cancer treatment and its prevention is a key factor in cancer prognosis. Approximately 80% of cancer patients still die from tumor dissemination following treatment by surgery, radiotherapy and chemical therapy; therefore, it is an urgent task to find new effective anti-metastatic drugs. Low-molecular-weight heparin (LMWH; e.g., enoxaparin, dalteparin, reviparin, and tinzaparin) and its mechanisms in tumor metastasis have been studied widely. Studies have shown that cancer patients who had been treated with LMWH for thrombosis had a significantly improved 3 to 6 month survival rate (Smorenburg et al., 1999; Smorenburg and Van Noorden, 2001; Akl EA et al., 2007). Animal studies have also shown that LMWH has an anti-metastatic effect on multiple neoplasms with improved animal survival rates (Mousa SA et al., 2006). LMWH influences both tumor cell and endothelial cell functions, including cell proliferation, adhesion, invasion, angiogenesis, and metastasis, and affects a wide range of molecules, such as vascular endothelial growth factor (VEGF), matrix metalloproteases (MMPs), heparinase, selectins, adhesion molecules, nuclear factor kappa B (NF-κB), and plasminogen. Tumor cell adhesion to, and migration through, the endothelial cell layer are both essential components of tumor metastasis (Kramer and Nicolson, 1979). The vascular endothelium constitutes an anatomical barrier between circulating tumor cells and extravascular tissues, and its integrity is important in maintaining this function (Kusama et al., 1995). Some reports have shown that LMWH can protect endothelial cells (EC) from activation and that it can inhibit the expression of cell

adhesion molecules when used as an anticoagulant in patients with coronary artery disease (Lindmark and Siegbahn, 2002; Manduteanu et al, 2002). We proposed that the protective effects of LMWH on endothelial cells could possibly also aid its anti-metastatic pharmacological actions.

In this study, we investigated (i) the effects of incubating endothelium with LMWH; and (ii) the adhesion to and migration through the endothelium of a type of tumor cell, high metastasis human prostate cancer cells (PC-3M), to analyze and confirm the effects of LMWH on tumor metastasis and to explore its molecular mechanisms.

Materials and Methods

Cell culture

Human umbilical vein endothelial cells (HUVECs) were isolated using collagenase I (1 mg/ml, Invitrogen) digestion of umbilical veins from undamaged sections of fresh cords. HUVECs were grown in M199 (Gibco) supplemented with 20% heat-inactivated fetal bovine serum (FBS), 20 μg/ml endothelial cell growth supplement (Sigma), 100 U/ml penicillin, 100 μg/ml streptomycin and 2 mM L-glutamine. The identification of HUVECs was confirmed by their polygonal morphology and by detection of their immunoreactivity for factor VIII-related antigens (Andrews et al., 2001). PC-3M cells were cultured in RPMI1640 medium containing 10% heat-inactivated FBS, 100 U/ml penicillin, and 100 μg/ml streptomycin in a humidified incubator with 5% CO_2 in air at 37°C.

Adhesion assay

PC-3M cells were labeled with CFDA (carboxyfluorescein diacetate, Sigma, 100 μg/ml) for 30 min at 37°C (Woodward et al., 2002). Cells were washed with phosphate-buffered saline (PBS) twice to remove residual fluorescent dye. Cell viability was not compromised by this labeling protocol, as indicated by trypan blue exclusion.

HUVECs were cultured in 96-well dishes coated with 1% gelatin. When HUVECs reached an approximate confluency of 80%, they were pretreated with 0.05–500 μg/ml heparin (LMWH; Sigma, deaminated sodium salt from porcine intestinal mucosa, low-molecular-weight mono-aldehyde, heparin >75 USP units/mg, average molecular weight 5 kDa) for 24 h; HUVECs were then cultured in fresh M199. CFDA-labeled PC-3M cells were washed and resuspended in culture medium (1×10^5 cells/ml). One hundred microliters of the tumor cell suspension were added to HUVEC monolayers in 96-well dishes and co-cultured with HUVECs for 30 min at 37°C. At the end of the incubation, wells were washed twice with PBS to remove non-adherent PC-3M cells. Adherent cells were counted under a fluorescence microscope using an excitation wavelength of 492 nm, and counts were performed in five fields in each well (Andrews et al., 2001).

Transendothelium migration assay

Cell migration was assayed using a modified Boyden chamber assay. Approximately

1×10^5 HUVECs were grown on a 5.0-μm pore gelatinized polycarbonate membrane that separated the two compartments of a 6.5-mm migration chamber (Transwell Costar). When HUVECs reached 80% confluency, they were treated with LMWH (0.05–500 μg/ml) for 24 h. Then, tumor cells in suspension (1×10^6 cells/ml) were added onto the HUVEC monolayers in the apical chamber and RPMI1640 containing 10 μg fibronectin (FN) was added to basolateral chamber. After incubation for 18 h, cells on the upper face of the membrane were scraped using a cotton swab and tumor cells that had migrated to the lower face of the filter were trypsinized and counted using a flow cytometer (BD-LSR, USA).

MTT assay

HUVECs were plated into 96-well dishes (1×10^4 cells/well) and incubated in M199 medium for 24 h. The culture medium was changed to a medium containing a range of concentrations of LMWH and incubated for 24 h. At the end of these treatments, 20 μl of sterile MTT dye (Sigma, USA) was added. Cells were incubated at 37°C for 2 h. After removing medium, 100 μl of dimethyl sulfoxide was added and thoroughly mixed. Spectrometric absorbance at 540 nm (for formazan dye) and 690 nm (as background level) was measured using a microplate reader (Bio-Rad, USA) (Tozawa et al., 2003).

Scanning electron microscopy (SEM) assay

SEM analysis was used to detect the effect of LMWH on morphological changes in

HUVECs when bound by PC-3M cells. Cell culture and drug incubation methods were similar to those used in the adhesion assay. After 30 min, the co-culture was rinsed and fixed in 37°C 3% glutaraldehyde in 0.1 M cacodylate buffer (pH 7.3) for 1.5 h. After fixation, cells were stored at 4°C in buffer until final processing, which was accomplished by dehydrating cells in a graded series of acetones and then drying out in liquid CO_2. Cells were coated with a thin layer of gold–palladium prior viewing under a JEOL JSM-5600LV SEM (JEOL, USA) (Douglas et al., 1999).

The measurement of intracellular Ca^{2+} in HUVECs

HUVECs were plated onto a confocal Petri dish (1×10^5 cells) and incubated with 50 μg/ml LMWH for 24 h. Confluent HUVEC monolayers were washed three times with M199 solution and loaded with 5 mM Fluo-3/AM (Molecular Probes, USA) in M199 for 1 h at 37°C and used for intracellular Ca^{2+} measurement (Minta et al., 1989; Lewalle et al., 1998). Tumor cells to be plated on Fluo-3-loaded HUVECs were detached using 0.1% ethylenediaminetetraacetic acid (EDTA) in PBS, and added to HUVEC monolayers at a final concentration of 5×10^3 cells in 50 μl per chamber. Ca^{2+}-dependent changes in fluorescence intensity were recorded continually in individual cells using a TCS-NT laser scanning confocal microscope (Leica, Germany) with an excitation wavelength of 490 nm.

Two-dimensional electrophoresis (2-DE)

After HUVECs reached sub-confluence, they were treated with 50 μg/ml LMWH for

24 h. Immediately after treatment, cells were placed on ice, washed with ice-cold PBS, suspended at a concentration of about 1×10^7 cells/ml and lysed with a buffer consisting of 40 mM Tris, 8 M urea, 4% w/v CHAPS, 60 mM dithiothreitol (DTT) and 1 mM phenylmethylsulfonyl fluoride (PMSF; Sigma). The protein concentration in lysates was measured using the Bradford method. Two samples (treated with or without LMWH) containing 55 µg of protein respectively were added to rehydration solution (8 M urea, 2% CHAPS, 0.5% immobilized pH gradients (IPG) buffer, 0.28% DTT and trace bromophenol blue). The final volume was 125 µl.

Isoelectric focusing (IEF) was performed in the initial dimension, using commercially available preformed immobilized pH gradients (linear pH gradient 3–10, 7 cm). Gels were rehydrated overnight by placing strips gel-side down in a solution that contained rehydration solution in an IPGphore strip holder (Amersham Pharmacia Biotech) and covered with mineral oil. IEF was conducted using an IPGphore Isoelectric Focusing System (Amersham Pharmacia Biotech). IEF was run at 20°C using the step-and-hold and gradient methods as follows: IPG strips were rehydrated with sample at 0 V for 6 h, then IEF was performed at 30 V for 6 h; linear increase to 200 V for 0.5 h; held at 500 V for 0.5 h; followed by 1000 V for 0.5 h; then at 8000 V for 4–5 h. Before second dimension electrophoresis (sodium dodecyl sulphate–polyacrylamide gel electrophoresis [SDS-PAGE]), the IEF strips were equilibrated for 15 min in solution (6 M urea, 30% glycerol, 50 mM Tris–HCl [pH 8.8[, 2% SDS) containing 10 mg/ml DTT for 15 min, and then for a further 15 min in equilibration solution containing 25 mg/ml iodoacetamide. SDS-PAGE was run in a

10% gel, without stacking gels, using the Pharmacia IsoDalt system. The IPG gel strips were embedded on top of the gels with 0.5% agarose. Electrophoresis was conducted at a constant current of 30 mA/gel. The protein isoelectric point (pI) and molecular weight, respectively, were assigned by calibration of 2D PAGE gels with carbamylyte pI calibration markers and molecular weight markers (Amersham Pharmacia Biotech, USA). Gels were stained with Coomassie blue. The experimental procedures were repeated three times. The differentially expressed protein spots were excised manually from the SDS–PAGE gels and subject to in-gel tryptic digestion.

Mass spectrometry identification of proteins

The protein spot of interest was analyzed by matrix-assisted laser desorption ionization time-of-flight mass spectrometry (MALDI-TOF-MS). The proteins from the selected spots were reduced with DTT and alkylated with iodoacetamide before overnight digestion with a sequence-grade modified trypsin (Promega, USA). The peptide mixture was concentrated and desalted using Millipore ZipTip m-C18 pipette tips. The peptide mass fingerprints were measured with a Bruker Inc Biflex III MALDI-TOF-MS in a positive ion reflector mode using a-cyano-4-hydroxycinnamic acid as a matrix. The database searches were performed using Mascot (www.matrixscience.com) searches.

Immunofluorescence assay

HUVECs were grown on glass coverslips in 5% CO_2 in air at 37°C and then

incubated in 50 µg/ml LMWH for another 24 h. Next, 3000 CFDA-labeled PC-3M cells were added to the coverslips and co-incubated with HUVECs for 30 min. After they were gently washed in PBS, the coverslips were fixed in 3.7% formaldehyde for 10 min. Then, the fixed cells were incubated with anti-human vimentin monoclonal antibodies (Clone V9, Neomarkers, USA) at 37°C in a humid chamber for at least 1 h, washed three times in PBS, and incubated with goat anti-mouse IgG TRITC- or FITC-conjugated secondary antibody for an additional 1 h at 37°C. For samples stained with FITC, HUVECs were incubated with 0.625 µg/ml propidium iodide (PI) for 15 min at room temperature. After several washes, stained specimens were viewed using a TCS-SP_2 laser scanning confocal microscope (Leica, Germany) (Gonzales et al., 2001).

Ribonucleic acid isolation and reverse transcription–polymerase chain reaction (RT-PCR)

HUVECs were grown to at least 80% confluency and then incubated in different concentrations of LMWH for another 24 h. Then total RNA was isolated using Trizol reagent (Invitrogen, Groningen, The Netherlands). A further set of samples were investigated as follows: HUVECs were grown to at least 80% confluency and then incubated with different concentrations of LMWH for a further 24 h. Next, PC-3M cells were added to the culture wells and co-incubated with HUVECs for 2 min. Total RNA was immediately isolated with the use of Trizol reagent. First-strand cDNAs were generated from RNA samples by reverse transcription using oligo(dT)s. The

JPET Fast Forward. Published on July 6, 2011 as DOI: 10.1124/jpet.111.182055
This article has not been copyedited and formatted. The final version may differ from this version.

following primers were used: β-actin F: 5′-ATCATGTTTGAGACCTTCAACA-3′ and R: 5′-CATCTCTTGCTCGAAGTCCA-3′; PP-1B F: 5′-CGTCCTGTCACTCCACCTC-3′ and R: 5′-TCCTTTACCCGTCTCCTTA-3′; vimentin F: 5′-GACAATGCGTCTCTGGCACGTCTT-3′ and R: 5′-TCCTCCGCCTCCTGCAGGTTCTT-3′; transforming growth factor-beta (TGF-β) F: 5′-CAAGTGGACATCAACGGTGAGG-3′ R: 5′TGGCCATGAGAAGCAGGAAAGG-3′; E-cadherin F: 5′-TGGAGGAATTCTTGCTTTGC-3′ R: 5′-CGTACATGTCAGCCAGCTTC-3′; and α_v integrin F: 5′-GACTGTGTGGAAGACAATGTCTGTAAACCC-3′, R: 5′-CCAGCTAAGAGTTGAGTTCCAGCC-3′.

Western blot analysis

Cell culture and drug levels were the same as that for the RT-PCR experiment. Total protein was extracted using RIPA lysis buffer. Equal amounts of protein were subjected to SDS–PAGE on a 10% polyacrylamide gel for the detection of vimentin. The membrane with blotted protein was blocked for 1 h with blocking buffer containing 5% non-fat dried milk and 0.05% Tween 20 in Tris-buffered saline (TBS-T), followed by incubation with anti-vimentin antibody (1:1000, Clone V9, Neomarkers, USA), which was diluted in blocking buffer overnight at 4°C. Then, the membrane was washed three times with TBS-T for 30 min and incubated at room temperature for 1 h with diluted (1:2000) secondary HRP-labeled IgG (Santa Cruz, CA, USA). Detection was done using the enhanced chemiluminescence (ECL)

JPET Fast Forward. Published on July 6, 2011 as DOI: 10.1124/jpet.111.182055
This article has not been copyedited and formatted. The final version may differ from this version.

method.

Short interfering ribonucleic acid (siRNA) transfection

siRNA duplexes used in this study were bought from Santa Cruz, to interfere with vimentin expression. Non-silencing siRNA (5′-UUAAGUAGCUUGGCCUUGATdT-3′ and 5′-UCAAGGCCAAGCUACUUAATdT-3′) was used as the negative controls. siRNA duplexes were transfected into HUVECs with siRNA transfection reagent (Polyplus-transfection Inc., San Marcos, CA, USA), according to the manufacturer's instructions. After transfection for 48 h, cells were subjected to Western blot analysis to detect the efficiency of vimentin knockdown following binding of PC-3M cells.

Surface plasmon resonance (SPR) studies

All chemicals, bovine serum albumin (BSA), and dimethyl sulfoxide (DMSO) were purchased from Sigma Chemical Co. (St. Louis, MO, USA). Biacore3000, CM5 series sensor chips, and coupling reagents (*N*-ethyl-*N*′-(3-dimethylaminopropyl) carbodiimide (EDC), *N*-hydroxysuccinimide (NHS) and ethanolamine–HCl) were purchased from Biacore AB (Uppsala, Sweden). LMWH was dissolved directly in HEPES-buffered saline (10 mM HEPES, 150 mM NaCl, pH 7.4).

CM5 sensor chips were placed in the instrument and preconditioned with water (100 μl/min) by applying two consecutive 50 μl/min pulses of 50 mM NaOH and 1 M NaCl, then 10 mM HCl and 0.1% SDS, and finally water. Vimentin protein (Sigma)

was immobilized onto CM5 sensor chips using amine-coupling chemistry in running buffer, which consisted of 10 mM HEPES, 150 mM NaCl, 3 mM EDTA and 0.005% surfactant P-20, pH 7.4 (HBS-EP). Vimentin at a concentration of 50 μg/ml in 10 mM sodium acetate, pH 5.2, was injected for 7 min, resulting in immobilized densities that averaged 2000–4000 RU. The surfaces were blocked with an 8-min injection of 1 M ethanolamine, pH 8.0. Prior to use, the surface coverage of vimentin on CM5 sensor chips was evaluated using anti-vimentin antibody (Clone V9, Neomarkers, USA) binding assay on CM5 sensor chips and vimentin immobilized CM5 sensor chips.

The binding assay was performed in HBS-EP running buffer at 25°C. LMWH was injected over the vimentin immobilized CM5 sensor chips and reference surfaces from 0.5 to 50 μg/ml in two-fold dilutions at a flow rate of 50 μl/min. Triplicate injections of each LMWH concentration were analysed in random order. The LMWH–vimentin complex was allowed to associate and dissociate for 60 s and 20 s, respectively, and the surfaces were washed with running buffer for 10 s between each sample injection. Buffer blanks were injected after LMWH for double referencing. Data were collected at a rate of 1 Hz.

All sensorgrams were processed by first subtracting the binding response recorded from the control surface (center reference spot), followed by subtracting an average of the buffer blank injections from the reaction spot.

Detection of fluorescently-labeled heparin inside HUVECs

To identify whether heparin could enter HUVECs through the cell membrane, we

incubated these cells with fluorescently-labeled heparin (Invitrogen, USA) for 24 h and 48 h. Then cells were washed three times with PBS to remove excess heparin. Next, an anti-vimentin antibody was used to show the cell morphology.

Statistical analysis

Each of these experiments was conducted in triplicate. Data are expressed as mean ± standard error of mean (S.E.M.). Statistical significance of differences between means was determined by one-way analysis of variance followed by Dunnett's test (SPSS 10.0 software). A p-value of <0.05 was considered to be statistically significant.

Results

Inhibitory effect of LMWH on PC-3M adhesion to HUVECs.

CFDA was used to label PC-3M cells in order to differentiate PC-3M cells from HUVECs under a 492 nm excitation wavelength. The viability of CFDA-labeled PC-3M cells was more than 95%. LMWH used at a concentration of between 0.5–500 μg/ml reduced the number of tumor cells that adhered to the HUVEC monolayer. The number of PC-3M cells found in the 50 μg/ml and 500 μg/ml LMWH groups (32 ± 1.6 and 30 ± 1.9 respectively) were significantly different ($p<0.01$) compared with that of the untreated control group (43 ± 4.9) (Fig. 1).

Under SEM, HUVECs were seen to form a monolayer with gaps of 10–20 nm between cells (Fig. 2A). Most tumor cells were seen to adhere to the boundary of the HUVECs, with fewer cells sticking to the HUVEC surface. The addition of PC-3M

cells caused shrinkage of the HUVECs such that the gaps between HUVECs widened (Fig. 2B). LMWH prevented HUVEC shrinkage when added at a concentration of 50 μg/ml (Fig. 2C).

Under SEM high magnification, the surfaces of normal HUVECs were seen to be smooth (Fig. 2D), but when PC-3M cells adhered to the surface of these cells breaks in the membranes could be seen with resulting leakage of cytoplast granules (Fig. 2E). In contrast, when HUVECs were treated with 50 μg/ml LMWH for 24 h their membrane surfaces were smoother than those of the untreated controls following PC-3M cell adhesion (Fig. 2F).

Inhibitory effect of LMWH on PC-3M cell transendothelial migration

Transwell chambers were used to assay the effect of LMWH on PC-3M cell transendothelial migration following tumor cell adhesion to HUVEC monolayers. Fibronectin was added into the basolateral chamber to function as a chemoattractant. PC-3M cells were co-incubated with HUVECs for 18 h; cells that migrated to the lower face of the filter were all shown to be PC-3M cells using factor VIII staining (data not shown). The pretreatment of HUVECs with LMWH for 24 h led to a dose-dependent decrease in the transendothelial migration of PC-3M cells across the HUVEC monolayers (Fig. 3). The number of PC-3M cells in the 50 and 500 μg/ml LMWH groups (8,700 ± 399 and 7,768 ± 328 cells, respectively) that migrated across the epithelium was greatly reduced ($p<0.01$) compared with that found for the control group (14,249 ± 1204 cells)

JPET Fast Forward. Published on July 6, 2011 as DOI: 10.1124/jpet.111.182055
This article has not been copyedited and formatted. The final version may differ from this version.

Effect of LMWH on viability of HUVECs

LMWH concentration did not influence HUVEC cell growth significantly following 24 h treatment (p>0.05; data not shown).

Effect of LMWH on PC-3M cells-induced $[Ca^{2+}]_i$ elevation in HUVECs

Other studies have found that endothelial cell intracellular Ca^{2+} concentration is increased following tumor cell contact and that this rise mediates tumor cell transendothelial migration (Lewalle et al., 1998). We measured the Ca^{2+} concentration in HUVECs that had been pre-treated with LMWH for 24 h to determine whether this treatment affected the level of intracellular calcium ions in HUVECs following PC-3M tumor cell adhesion. PC-3M cell-induced $[Ca^{2+}]_i$ change in HUVECs was expressed as relative fluorescence density (F_t/F_0), in which F_0 is the initial fluorescence density of each cell, and F_t is the real-time fluorescence density of the same cell after addition of tumor cells. When quiescent, HUVEC monolayers had a weak Ca^{2+} signal that was detected in the cytoplasm and that remained stable for several hours in the assay buffer (Fig. 4A). The addition of PC-3M to the HUVEC monolayers induced an immediate and marked elevation in HUVEC $[Ca^{2+}]_i$ with a maximal increase of 220% of relative fluorescence intensity that was reached within 20 s following PC-3M contact with HUVECs (Fig. 4B). When we used PC-3M conditioned medium, no elevation in HUVEC $[Ca^{2+}]_i$ was observed (data not shown). The $[Ca^{2+}]_i$ levels then decreased slowly to the basal level within 200–220 s (Fig. 4G).

JPET Fast Forward. Published on July 6, 2011 as DOI: 10.1124/jpet.111.182055
This article has not been copyedited and formatted. The final version may differ from this version.

In HUVECs that were pre-treated with 50 μg/ml and 500 μg/ml LMWH, before PC-3M addition there is a weaker Ca^{2+} signal similar to that of carrier-treated group (Figs. 4C and 4E); after the addition of PC-3M to the HUVEC monolayers induced a slow and delayed elevation in $[Ca^{2+}]_i$ (Figs. 4D and 4F). For HUVECs pre-treated with 50 μg/ml and 500 μg/ml LMWH, respectively, this elevation in $[Ca^{2+}]_i$ almost completely abated and the maximal increase of relative fluorescence intensity of HUVEC $[Ca^{2+}]_i$ was approximately 170% and 140%, respectively ($p<0.01$ compared with the carrier group; Fig. 4G).

Comparative proteomic analysis in HUVECs with or without LMWH treatment

Schematic representations of both control and treated 2-DE protein patterns are shown in Fig. 5A, which shows over 150 Coomassie blue-stained protein spots, with most spots in the pH 4–7 region. The protein profile of carrier-treated and LMWH-treated HUVECs was compared using computer-assisted analysis of the respective Coomassie-stained spot patterns; 43 protein spots were found to alter their expression level in response to LMWH exposure.

Four spots that were significantly affected by LMWH treatment were subjected to tryptic digestion and MALDI-TOF/MS analysis. Of these four spots, two marked as C111 and C125 had a decrease in intensity; the other two protein spots, marked as L38 and L141, increased in intensity after LMWH treatment. The data obtained from MALDI-TOF-MS (Fig. 5B–E) were applied to the protein database and searches were performed to determine the identity of the four proteins or peptides. Our results

showed that protein spots C111 and C125 might be vimentin, protein components of class III-intermediate filaments; protein spot L38 might be a C-type lectin superfamily member 1 precursor (cartilage-derived C-type lectin) fragment; and protein spot L141 might be serine/threonine protein phosphatase PP1-beta catalytic subunit fragment. We confirmed this change using immunofluorescence chemistry, western blot and RT-PC analysis and investigated the function of vimentin in LMWH's anti-adhesion effect on HUVECs and PC-3M cells using vimentin siRNA.

Effects of LMWH on vimentin redistribution in HUVECs and PC-3M cell adhesion

We decided to look at changes in vimentin expression and redistribution in HUVECs and on PC-3M cell adhesion after 30 min to investigate the mechanisms of the LMWH effects on endothelium and PC-3M cell adhesion and migration.

Carrier-treated HUVECs presented a finely stained intracellular vimentin network that radiated homogeneously from the perinuclear area to the cell periphery (Fig. 6A, C). LMWH-treated HUVECs presented no dramatically different distribution pattern when compared with the control, with only a slight change in vimentin filaments (Fig. 6B).

When PC-3M cells were added to the HUVECs, the vimentin in the HUVECs showed significant filament bundling and collapsed intermediate filaments (Fig. 6D). LMWH-treated HUVECs could alleviate this change and presented a more normal radial pattern. (Fig. 6E)

JPET Fast Forward. Published on July 6, 2011 as DOI: 10.1124/jpet.111.182055
This article has not been copyedited and formatted. The final version may differ from this version.

Effects of LMWH on vimentin protein and vimentin-related genes expression in HUVECs and PC-3M cell adhesion

Following incubation of HUVECs with LMWH (50 and 500 μg/ml) for 24 h, there was an increase tendency in E-cadherin and TGF-β gene expression and a decrease in PP-1B and α_v integrin gene expression. LMWH at the concentration of 500 μg/ml could significantly inhibit the mRNA expression of α_v integrin ($p<0.05$). In contrast, expression of vimentin only decreased by a small amount, and this was only observed at the higher dose (500 μg/ml) (Fig. 6F). For HUVECs with bound PC-3M cells, LMWH at the 50 μg/ml concentration could inhibit the expression of PP-1B and α_v integrin significantly ($p<0.05$; Fig. 6G).

Vimentin-targetted siRNA in HUVECs reduced PC-3M cell adhesion to endothelium

When HUVECs were transfected with siRNA against the vimentin gene for 48 h, the expression of vimentin in HUVECs was partially reduced by 25% in comparison to the controls ($p<0.05$; Fig. 7A) and the adhesion of PC-3M cells to HUVECs was reduced to approximately 16% the value of the control, that is the number of adherent tumor cells to HUVECs decreased from 67 ± 5 in controls to 56 ± 4 in siVimentin ($p<0.05$; Fig. 7B).

Binding of LMWH to vimentin by SPR

SPR biosensor technology was utilized to detect the association and dissociation of

JPET Fast Forward. Published on July 6, 2011 as DOI: 10.1124/jpet.111.182055
This article has not been copyedited and formatted. The final version may differ from this version.

LMWH to vimentin in real time. Sensorgrams were processed using automatic correction for non-specific bulk refractive index effects. Figure 8A shows a typical sensorgram obtained by using LMWH concentrations of 0.5 to 50 μg/ml, which had been corrected for the response due to refractive index differences between running buffer and sample solution by subtracting the respective curves from a reference channel. We found that LMWH treatment resulted in a significant and dose-dependent increase in SPR response units (RU). The LMWH concentration series were fitted to a one-to-one binding with a mass-transfer model encoded in the Biacore 3000 evaluation software for binding affinity determination.

Drug distribution of fluorescently-labeled heparin in HUVECs

When fluorescently labeled heparin were added to HUVEC-conditioned medium for 24 h, confocal imaging showed us that most of this heparin was located around the cell membrane with only a small amount of heparin inside the cells. When this incubation was extended to 48 h, confocal imaging showed that several heparin particles had entered some cells and was mainly found in the cytoplasm (Fig. 8B).

Discussion

The intact endothelium can serve as a ‘defensive barrier’ to the extravasation of tumor cells (Lewalle et al., 1997; Lee et al., 2003). In the present study, we incubated HUVECs with LMWH for 24 h prior to the addition of PC-3M cells. We found that both adhesion of PC-3M cells to HUVECs and tumor cell transendothelial migration

JPET Fast Forward. Published on July 6, 2011 as DOI: 10.1124/jpet.111.182055
This article has not been copyedited and formatted. The final version may differ from this version.

in vitro were inhibited by the incubation of HUVECs with LMWH. We therefore proposed that LMWH protected the HUVECs from damage caused by PC-3M cells and enhanced the role of endothelium as a barrier against the extravasation of tumor cells (Lewalle et al., 1997; Lee et al., 2003). We found that LMWH-treated HUVECs adhered to by PC-3M cells had enhanced endothelial integrity under SEM. Furthermore, the incubation with LMWH could reduce the level of HUVEC stimulation by inhibiting the rise in Ca^{2+} ions that occurred when PC-3M tumor cells bound to the HUVEC cell surface.

Malignant tumor cells can transiently increase the calcium concentration of endothelial cells in the contact area and stimulate endothelial cell retraction by disrupting the intercellular junctions and promoting the transendothelial migration of tumor cells (Lewalle et al., 1998; Lee et al., 2003). This rapid increase of $[Ca^{2+}]_i$ in HUVECs stimulated by PC-3M cells was inhibited when HUVEC monolayers alone were treated with LMWH. Intracellular Ca^{2+} movement is part of a signal transduction pathway that is initiated by the contact between tumor cells and endothelial cells. Transient changes in endothelial $[Ca^{2+}]_i$ may have persistent effects and mediate multiple steps in the transendothelial migration of tumor cells. The effect of these on interendothelial cohesion and levels of cytosolic free Ca^{2+} may modulate the presence of various ligands on the endothelial cell surface, including lectins, intercellular adhesion molecules (ICAMs) and integrins (Pili et al., 1993). Furthermore, Ca^{2+} may stimulate the secretion of chemoattractant and/or motility factors, which then stimulate tumor cell transendothelial migration. Timar et al. found

that calcium channel blockers (nifedipine, verapamil, and diltiazem) could inhibit the interaction between tumor cells and platelets; they postulated that tumor cell metastasis is due not only to the effects of the Ca^{2+} channel blockers on platelets, but also to their effect on the tumor cell cytoskeleton, including vimentin intermediate filaments. This results in the inhibition of the mobility and function of the alpha IIb beta 3 receptor (Timar et al., 1992).

Furthermore, Ca^{2+} signals activate Ca^{2+}/calmodulin dependent protein kinase II (CaMKII), which has been reported to be one of the kinases that phosphorylate vimentin in vitro. Thus, the amplitude and duration of an extracellular stimulation are likely to coordinate the spatially-organized phosphorylation of vimentin filaments through the Ca^{2+}-CaM-CaMKII-vimentin signaling pathway (Inagaki et al., 1997). The structural organization of vimentin was strongly disrupted in the presence of the calcium-channel blocker, and increased concentrations of calcium channel blocker could reduce the levels and assembly of vimentin phosphate. Therefore, we deduced that the inhibition of $[Ca^{2+}]_i$ rise was involved during the modulation of vimentin morphology by LMWH in HUVECs (Retrosen and Gallin, 1986; Erhinger et al, 1996).

Vimentin is a protein that is altered by the effects of LMWH on HUVECs, which we detected with the use of the 2DE methodology. Using IFC, we found that the structure of vimentin on HUVECs was altered greatly by the addition of PC-3M cells; vimentin in the HUVECs showed significant filament bundling and collapsed intermediate filaments; however, the resulting fusion of the cytoskeleton vimentin

intermediate filament could be prevented greatly by a prior incubation of the HUVECs with LMWH for 24 h.

Vimentin intermediate filaments, in addition to their potential interactions with microfilaments and microtubules, participate in many other specialized cell functions. These include functioning as the cytoplasmic organizer, a supracellular mechanical scaffold, intercellular transporter, and signal transducer (Tang *et al*, 1993; Asaga *et al*, 1998). Several groups have recently reported that, in endothelial cells, vimentin controls directly or indirectly the cell–cell contact area and stabilizes cell–matrix adhesion (Tsuruta and Jones, 2003). Vimentin has a key role in adhesion through regulation of integrin functions. It has been reported that vimentin co-localises with adhesion plaques to stabilize the plaque. Adhesion plaque formation therefore influences cell–cell adhesion (Bershadsky et al., 1987; Burridge et al., 1988). In our present experiment, the structural organization of vimentin in endothelial cells by LMWH could therefore play an important role in the anti-adhesion and anti-transendothelial migration functions of LMWH. Our results of vimentin-targetted siRNA showed that partial knockdown of vimentin in HUVECs could reduce the ability of PC-3M cells to bind to HUVECs. We also ascertained that α_v integrin alone was downregulated in HUVECs pre-incubated with LMWH and in HUVECs after addition of PC-3M cells. Therefore, we concluded that vimentin and α_v integrin is involved in the molecular mechanism of LMWH inhibition on PC-3M cell adhesion to and migration through the endothelium.

Interestingly, SPR studies, which are used to detect molecular binding patterns,

have shown that, as well as the regulation of the expression and structure of vimentin by LMWH, there is direct interaction between LMWH and vimentin when purified vimentin protein is used. Binding by the multi-hydroxyl molecule heparin may be the reason that it affects cellular vimentin, as previous findings have shown that heparin could binds to heparin sulphate on cell membranes and then has multiple biological activities. Does this direct binding between these molecules take place in cells? Therefore, we used fluorescently-labeled heparin to determine whether heparin could exist in cells and binding with cytosolic vimentin. Incubation of HUVECs with fluorescently-labeled heparin for 24 h showed that most of the heparin was not present inside the cell membrane. Therefore we concluded that direct binding of heparin with vimentin was low or non-existant for cells that underwent a 24 h incubation with fluorescently-labeled heparin. However, LMWH can regulate vimentin, possibly via cell membrane molecules, such as tyrosine kinases, heparin-binding proteins, or even inositol phosphate $(IP)_3$ receptors, rather than by direct intracellular binding with vimentin.

Besides vimentin, we reconfirmed that the levels of PP-1B decreased with the 2DE experiment, while TGF-β and E-cadherin gene expression levels increased. PP-1B is another protein whose gene expression was found to be influenced by LMWH in HUVECs. Protein serine/threonine phosphatase-1 (PP-1) is a major phosphatase that can directly dephosphorylate proteins, such as AKT, in order to modulate their activation and regulate the expression of downstream genes. It may be related with the inhibitory effect of heparin on tumor growth as other studies have

reported; PP-1 can promote cell survival and modulate cell differentiation (Xiao et al., 2010). TGF-β has profound effects on all cell types that comprise the vasculature, including endothelial cells. TGF-β inhibits both the proliferation and migration of endothelial cells in monolayer cultures in vitro (Roberts et al., 1989). E-cadherin, which is one of the most widely studied tumor suppressors in many kinds of cancers, belongs to a family of calcium-dependent cell adhesion molecules. The loss of E-cadherin expression has been reported to induce epithelial-mesenchymal transition in several cancers (Baranwal et al., 2009). We deduced that the increase of E-cadherin in HUVECs after incubation with LMWH was beneficial for endothelial cells in terms of its anti-adhesive and anti-transendothelial migration properties.

In conclusion, in this study we have demonstrated that LMWH effectively inhibits PC-3M cell binding to, and migration across, endothelium by regulating endothelial calcium ions, vimentin and by the further downregulation of integrins.

Authorship Contribution

Participated in research design: Y. Pan, Zhang, Xiao, Yu, Li.

Conducted experiments: Y. Pan, Lei, Han, Wang.

Contributed new reagents or analytic tools: Y. Pan, Lei, Teng, Liu, Yu, Ren.

Performed data analysis: Y. Pan, Zhang, Xiao, Wang, X. Pan.

Wrote or contributed to the writing of the manuscript: Y. Pan, An, Li.

References

Akl EA, van Doormaal FF, Barba M, Kamath G, Kim SY, Kuipers S, Middeldorp S, Yosuico V, Dickinson HO and Schünemann HJ (2007) Parenteral anticoagulation for prolonging survival in patients with cancer who have no other indication for anticoagulation. *Cochrane Database Syst Rev* **3:** CD006652.

Andrews EJ, Wang JH, Winter DC, Laug WE and Redmond HP (2001) Tumor cell adhesion to endothelial cells is increased by endotoxin via an upregulation of β-1 integrin expression. *J Surg Res* **97:** 14–19.

Asaga H, Yamada M and Senshu T (1998) Selective deimination of vimentin in calcium ionophore-induced apoptosis of mouse peritoneal macrophages. *Biochem Biophys Res Commun* **243:** 641–646.

Bershadsky AD, Tint IS and Svitkina TM (1987) Association of intermediate filaments with vinculin-containing adhesion plaques of fibroblasts. *Cell Motil Cytoskeleton* **8:** 274–283.

Baranwal S, Alahari SK. (2009) Molecular mechanisms controlling E-cadherin expression in breast cancer.*Biochem Biophys Res Commun* **384**:6-11

Burridge K, Fath K, Kelly T, Nuckolls G and Turner C (1988) Focal adhesions: transmembrane junctions between the extracellular matrix and the cytoskeleton. *Annu Rev Cell Biol* **4:** 487–525.

Douglas GC, Thirkill TL and Blankenship TN (1999) Vitronectin receptors are expressed by macaque trophoblast cells and play a role in migration and adhesion to endothelium. *Biochim Biophys Acta* **1452:** 36–45.

Erhinger WD, Edwards MJ and Miller FN (1996) Mechanisms of α-thrombin, histamine, and bradykinin induced endothelial permeability. *J Cell Physiol* **167:** 562–569.

Gonzales M, Weksler B, Tsuruta D, Goldman RD, Yoon KJ, Hopkinson SB, Flitney FW and Jones JC (2001) Structure and function of a vimentin-associated matrix adhesion in endothelial cells. *Mol Biol Cell* **12:** 85–100.

Inagaki N, Nishizawa M and Inagaki M (1997) Regulation of intermediate filament structures by cell signaling. *Aichi Cancer Cent Res Inst Sci Rep* **1996–1997:** 5–9.

Kramer RH and Nicolson GL (1979) Interactions of tumor cells with vascular endothelial cell monolayers: a model for metastatic invasion. *Proc Natl Acad Sci USA* **76:** 5704–5708.

Lee TH, Avraham HK, Jiang S and Avraham S (2003) Vascular endothelial growth factor modulates the transendothelial migration of MDA-MB-231 breast cancer cells through regulation of brain microvascular endothelial cell permeability. *J Biol Chem* **278:** 5277–5284.

Lewalle JM, Bajou K, Desreux J, Mareel M, Dejana E, Noel A and Foidart JM (1997) Alteration of interendothelial adherens junctions following tumor cell–endothelial cell interaction in vitro. *Exp Cell Res* **237:** 347–356.

Lewalle JM, Cataldo D, Bajou K, Lambert CA and Foidart JM (1998) Endothelial cell intracellular Ca^{2+} concentration is increased upon breast tumor cell contact and mediates tumor cell transendothelial migration. *Clin Exp Metastasis* **16:** 21–29.

Lindmark E and Siegbahn A (2002) Tissue factor regulation and cytokine expression

in monocyte–endothelial cell co-cultures. Effects of a statin, an ACE-inhibitor and a low-molecular-weight heparin. *Thromb Res* **108:** 77–84.

Manduteanu I, Voinea M, Capraru M, Dragomir E and Simionescu M (2002) A novel attribute of enoxaparin: inhibition of monocyte adhesion to endothelial cells by a mechanism involving cell adhesion molecules. *Pharmacology* **65:** 32–37.

Minta A, Kao PY and Tsien RY (1989) Fluorescent indicators for cytosolic calcium based on rhodamine and fluorescein chromophores. *J Biol Chem* **264:** 8171–8178.

Mousa SA, Linhardt R, Francis JL, and Amirkhosravi A (2006) Anti-metastatic effect of a non-anticoagulant low-molecular-weight heparin versus the standard low-molecular-weight heparin, enoxaparin. *Thromb Haemost* **96:** 816–821.

Pili R, Corda S, Passaniti A, Ziegelstein RC, Heldman AW, Capogrossi MC (1993) Endothelial cell Ca^{2+} increases upon tumor cell contact and modulates cell–cell adhesion. *J Clin Invest* **92:** 3017–3022.

Retrosen D and Gallin JI (1986) Histamine type I receptor occupancy increases endothelial cytosolic calcium, reduces F-actin, and promotes albumin diffusion across cultured endothelial monolayers. *J Cell Biol* **103:** 2379–2387.

Smorenburg SM, Vink R, te Lintelo M, Tigchelaar W, Maas A, Buller HR and van Noorden CJ (1999) In vivo treatment of rats with unfractionated heparin (UFH) or low molecular weight heparin (LMWH) does not affect experimentally induced colon carcinoma metastasis. *Clin Exp Metastas* **17:** 451–456.

Smorenburg SM and van Noorden CJ (2001) The complex effects of heparins on cancer progression and metastasis in experimental studies. *Pharmacol Rev* **53:**

93–105.

Tang DG, Timar J, Grossi IM, Renaud C, Kimler VA, Diglio CA, Taylor JD and Honn KV (1993) The lipoxygenase metabolite, 12(S)-HETE, induces a protein kinase C-dependent cytoskeletal rearrangement and retraction of microvascular endothelial cells. *Exp Cell Res* **207:** 361–375.

Timar J, Chopra H, Rong X, Hatfield JS, Fligiel SE, Onoda JM, Taylor JD and Honn KV (1992) Calcium channel blocker treatment of tumor cells induces alterations in the cytoskeleton, mobility of the integrin alpha IIb beta 3 and tumor-cell-induced platelet aggregation. *J Cancer Res Clin Oncol* **118:** 425–434.

Tozawa K, Kawai N, Hayashi Y, Sasaki S, Kohri K and Okamoto T (2003) Gold compounds inhibit adhesion of human cancer cells to vascular endothelial cells. *Cancer Lett* **196:** 93–100.

Tsuruta D and Jones JC(2003)The vimentin cytoskeleton regulates focal contact size and adhesion of endothelial cells subjected to shear stress. *J Cell Sci* **116** (Pt 24):4977-84.

Woodward JK, Nichols CE, Rennie IG, Parsons MA, Murray AK and Sisley K (2002) An in vitro assay to assess uveal melanoma invasion across endothelial and basement membrane barriers. *Invest Ophthalmol Vis Sci* **43:** 1708–1714.

Xiao L, Gong LL, Yuan D, Deng M, Zeng XM, Chen LL, Zhang L, Yan Q, Liu JP, Hu XH, Sun SM, Liu J, Ma HL, Zheng CB, Fu H, Chen PC, Zhao JQ, Xie SS, Zou LJ, Xiao YM, Liu WB, Zhang J, Liu Y and Li DW (2010) Protein phosphatase-1 regulates Akt1 signal transduction pathway to control gene expression, cell

survival and differentiation. *Cell Death Differ* **9**:1448-62.

Roberts AB and Sporn MB (1989) Regulation of endothelial cell growth, architecture, and matrix synthesis by TGF-beta. *Am Rev Respir Dis* **140**:1126-8.

Footnotes

This work was supported by grants from the National Natural Science Foundation of China [Nos. 81020108031, 30572202, 30973558, 30772571, 30901803 and 30901815]; the Major Specialized Research Fund from the Ministry of Science and Technology in China [No. 2009ZX09103-144]; the Research Fund from Ministry of Education of China (111 Projects) [No. B07001]; and the Scientific Research Foundation for the Returned Overseas Chinese Scholars, State Education Ministry, China.

Legends for Figures

Fig. 1. Inhibition of PC-3M cell adhesion to human umbilical vein endothelial cell (HUVEC) monolayers by low-molecular-weight heparin (LMWH). After 24 h exposure of HUVEC monolayers to PBS control (A), 5 μg/ml LMWH (B), 50 μg/ml LMWH (C), and 500 μg/ml LMWH (D), PC-3M cells labeled with 6-carboxyfluorescein diacetate (6-CFDA) were added onto HUVEC monolayers for 30 min; wells were washed twice with PBS to remove any non-adherent PC-3M cells, and the number of adherent PC-3M cells were then counted under a fluorescence microscope using an excitation wavelength of 492 nm. Five fields were counted in each well (E). Mean ± S.E.M. $n = 6$, $^*p < 0.05$ compared with control; magnification ×400, one field in each well. Each experiment was repeated in triplicate.

Fig. 2. Scanning electron micrograph analysis. After the adhesion of PC-3M cells to the human umbilical vein endothelial cell (HUVEC) monolayer for 30 min, the co-culture was rinsed, fixed and processed for scanning electron microscopy (SEM) assay. (A) Mono-cultured HUVECs with gaps of 10–20 nm between cells; (B) PC-3M cell adhesion to carrier-treated HUVECs. Spherical PC-3M cells were seen adhering to the boundary of the flattened HUVECs and caused shrinkage of the HUVECs; (C) PC-3M cell adhesion to 50 μg/ml low-molecular-weight heparin (LMWH)-treated HUVECs; (D) morphology of normal HUVECs with smooth surface; (E) morphology of carrier-treated HUVECs with bound spherical PC-3M cells and there were breaks in the membranes with a resulting leakage of cytoplast granules; (F) morphology of

JPET Fast Forward. Published on July 6, 2011 as DOI: 10.1124/jpet.111.182055
This article has not been copyedited and formatted. The final version may differ from this version.

50 μg/ml LMWH-treated HUVECs with bound spherical PC-3M cells. PC-3M cells are demonstrated with white arrows.

Fig. 3. Low-molecular-weight heparin (LMWH) inhibits the transendothelial migration of PC-3M cells across human umbilical vein endothelial cell (HUVEC) monolayers. HUVECs were cultured on 24-well transwell inserts with 5.0-μm pore gelatinized polycarbonate membranes and pre-treated with carrier (control) or LMWH (0.5–500 μg/ml) for 24 h. PC-3M cells were added to the HUVEC monolayers in the apical chamber. RPMI 1640 containing 10 μg fibronectin (FN) was added to the basolateral chamber. After incubation for 18 h, the number of PC-3M cells that migrated across the endothelial monolayers was counted by flow cytometry. Mean ± S.E.M. n =3, *p < 0.05 and **p < 0.01 compared with control. Each experiment was repeated in triplicate.

Fig. 4. Inhibitory effect of low-molecular-weight heparin (LMWH) on PC-3M cell-induced $[Ca^{2+}]_i$ elevation in human umbilical vein endothelial cells (HUVECs). HUVEC monolayers pre-treated with carrier (A,B), 50 μg/ml LMWH (C,D) or 500 μg/ml LMWH (E,F) were loaded with Fluo-3/AM. Changes in $[Ca^{2+}]_i$ were recorded in individual endothelial cells following the addition of PC-3M cells for 5 min. $[Ca^{2+}]_i$ levels in endothelial cells following the addition of PC-3M cells are shown in (B,D,F); the addition of PC-3M cells are indicated by the arrow in (G). The PC-3M cell-induced $[Ca^{2+}]_i$ changes in HUVECs are expressed as relative

fluorescence density (F_t/F_0), in which F_0 is the initial fluorescence density of each cell. F_t is the real-time fluorescence density of the same cell after the addition of tumor cells. Each experiment was repeated in triplicate. Mean ± S.E.M. $n = 3$, $^*p < 0.05$ and $^{**}p < 0.01$ compared with carrier group.

Fig. 5. Two-dimensional electrophoresis of human umbilical vein endothelial cell (HUVEC) proteins before and after low-molecular-weight heparin (LMWH) treatment with marked spots selected for matrix-assisted laser desorption ionization time-of-flight mass spectrometry (MALDI-TOF-MS). (A) Representative 2-dimensional electrophoresis maps of proteins in HUVECs without or with LMWH treatment. Approximately 55 μg total of protein was focused on linear immobilized pH gradient (IPG) strips (pH 3–10, 7 cm) before separating by 10% sodium dodecyl sulphate–polyacrylamide gel electrophoresis (SDS-PAGE). Coomassie blue staining was used to detect protein spots. Experiments were conducted in triplicate. (B,C) MALDI-TOF-MS analysis of protein C111 and C125 mass spectrometry of in-gel trypsin digests of this protein resulted in the identification of vimentin. (D) MALDI-TOF-MS analysis of protein L38 mass spectrometry of in-gel trypsin digests of this protein resulted in the identification of C-type lectin superfamily member 1 precursor (cartilage-derived C-type lectin) fragment. (E) MALDI-TOF-MS analysis of protein L141 mass spectrometry of in-gel trypsin digests of this protein resulted in the identification of serine/threonine protein phosphatase PP1-beta catalytic subunit fragment.

JPET Fast Forward. Published on July 6, 2011 as DOI: 10.1124/jpet.111.182055
This article has not been copyedited and formatted. The final version may differ from this version.

Fig. 6. The effects of low-molecular-weight heparin (LMWH) on vimentin distribution and expression in human umbilical vein endothelial cells (HUVECs) and PC-3M cell adhesion. Immunostaining of vimentin (green) in carrier-treated (A) and low-molecular-weight heparin (LMWH)-treated (B) HUVECs. Vimentin was detected by indirect immunofluorescence using a specific antibody and a FITC-labeled second antibody. Nuclei (red) were stained with propidium iodine (PI). To study the effect of LMWH on vimentin redistribution in HUVECs bound by PC-3M cells, HUVECs were grown to 80% confluency and then incubated with 50 μg/ml LMWH for 24 h. Next, 3,000 CFDA-labeled PC-3M cells (green) were added to the coverslips and co-incubated with HUVECs for 2 h. Then the co-cultured cells were labeled by vimentin staining and TRITC-conjugated secondary antibody (red). (C) Carrier-treated HUVECs, as in (A). (D) HUVECs with PC-3M binding. (E) LMWH-treated HUVECs and PC-3M cell binding. Next, reverse transcription-polymerase chain reaction (RT-PCR) analyses of human umbilical vein endothelial cells (HUVECs) with different concentrations of LMWH incubation for 24 h (F) and LMWH-treated HUVECs plus PC-3M cells for 2 min (G). Total RNA was isolated from cells using Trizol reagent. Each experiment was repeated in triplicate. Mean ± S.E.M. $n = 3$, $*p < 0.05$ compared with either the carrier-treated control group or the carrier-treated HUVECs bound with PC-3M cells group.

Fig. 7. siRNA interferes with vimentin expression. Non-silencing siRNA (ns-siRNA) was used as a negative control. Vimentin-targeted siRNA (siVimentin) was transfected into human umbilical vein endothelial cells (HUVECs) for 48 h; the total protein was extracted with protein lysis buffer and protein concentrations were measured using the Bradford protein assay. Cell lysates were analyzed by Western blotting using the vimentin antibody to detect the efficiency of vimentin knockdown (A). The effect of this vimentin knockdown on adhesion followed by PC-3M cells (B). Experiments were conducted in triplicate. Values shown are the mean ± S.E.M. of three experiments. *$p < 0.05$ vs. the control group.

Fig. 8. (A) Binding curves monitored on a surface containing 2,300 response units (RU) of immobilized vimentin and a range of LMWH concentrations (from top: 50, 5, 0.5 μg/ml). The curves are overlaid by calculated curves resulting from the fit of the experimental curves using a kinetic model considering one-to-one complex formation. **(B)** Human umbilical vein endothelial cells (HUVECs) incubated with fluorescently labeled heparin (green) for 24 h and 48 h. Vimentin (red) was labeled with anti-vimentin antibody to show the morphology of the cell cytoskeleton. Experiments were conducted in triplicate.

JPET Fast Forward. Published on July 6, 2011 as DOI: 10.1124/jpet.111.182055
This article has not been copyedited and formatted. The final version may differ from this version.

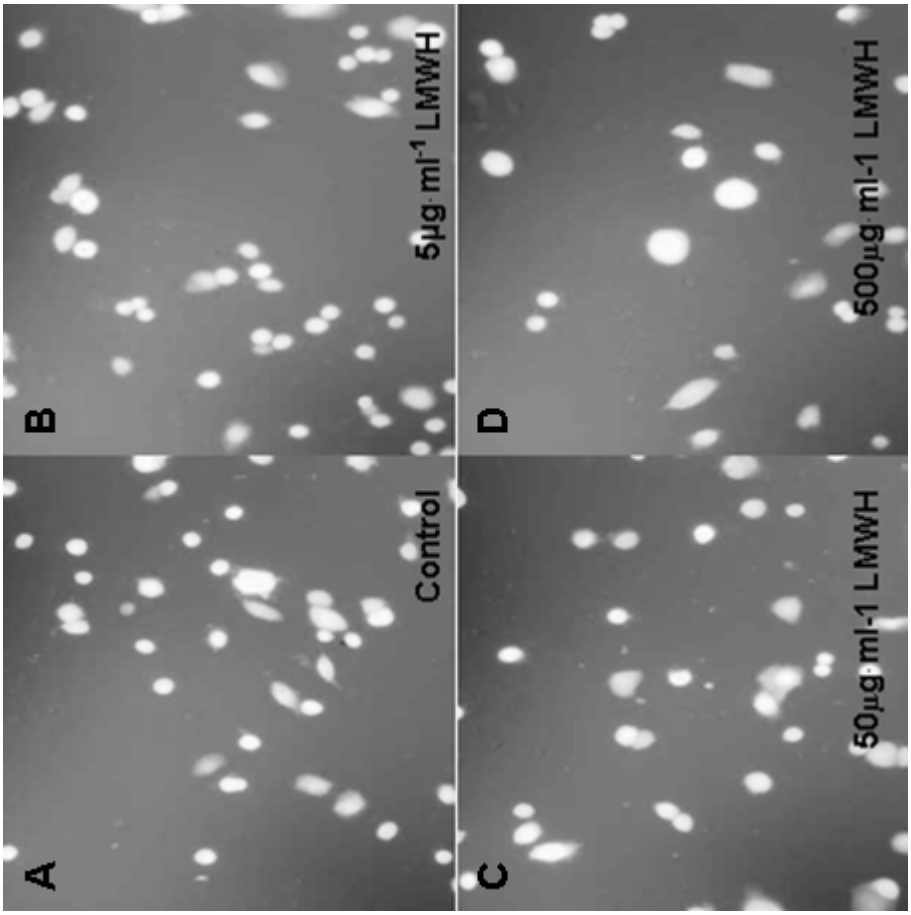

Fig. 1

JPET Fast Forward. Published on July 6, 2011 as DOI: 10.1124/jpet.111.182055
This article has not been copyedited and formatted. The final version may differ from this version.

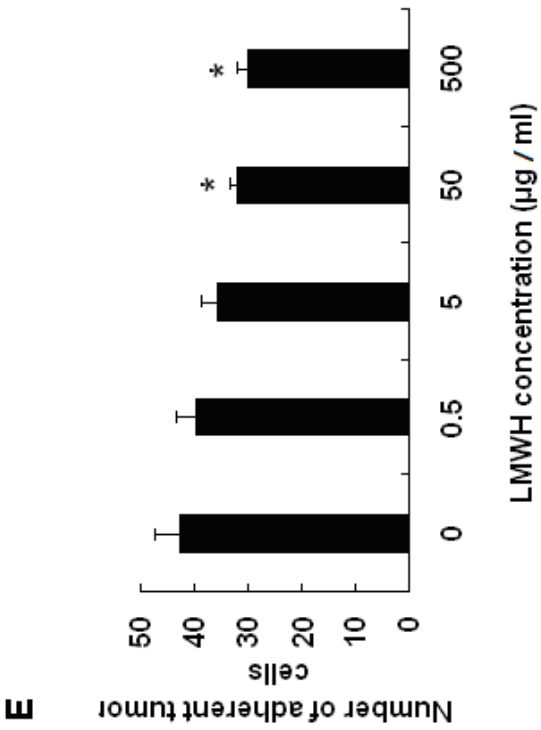

JPET Fast Forward. Published on July 6, 2011 as DOI: 10.1124/jpet.111.182055
This article has not been copyedited and formatted. The final version may differ from this version.

Fig. 2

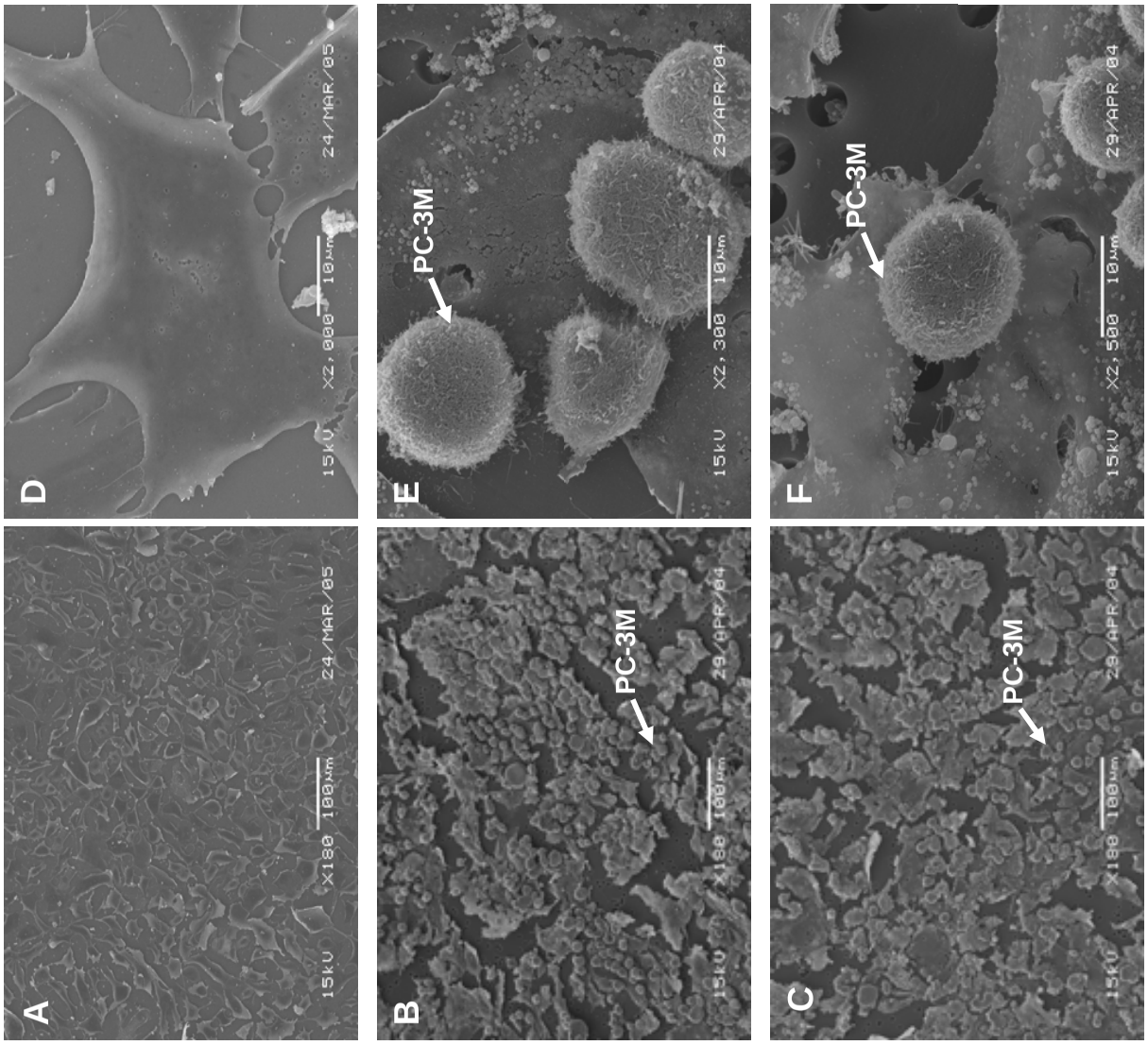

JPET Fast Forward. Published on July 6, 2011 as DOI: 10.1124/jpet.111.182055
This article has not been copyedited and formatted. The final version may differ from this version.

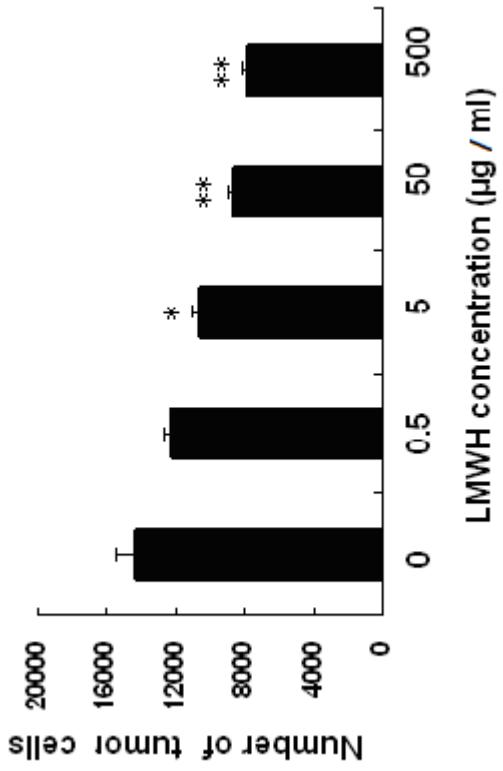

Fig. 3

JPET Fast Forward. Published on July 6, 2011 as DOI: 10.1124/jpet.111.182055
This article has not been copyedited and formatted. The final version may differ from this version.

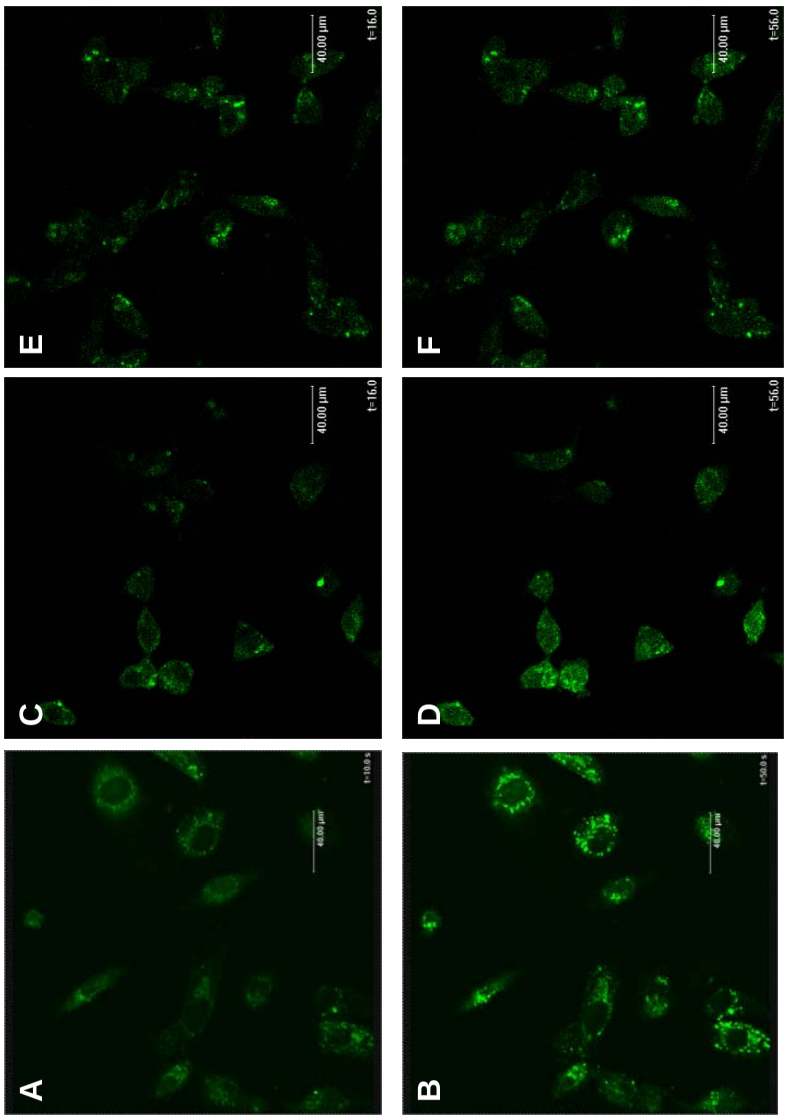

Fig. 4

JPET Fast Forward. Published on July 6, 2011 as DOI: 10.1124/jpet.111.182055
This article has not been copyedited and formatted. The final version may differ from this version.

G

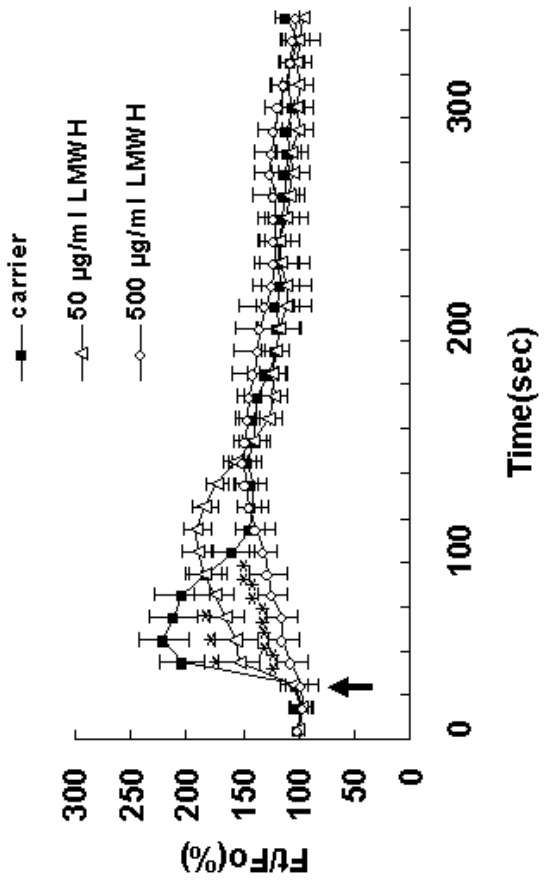

Fig. 5

A

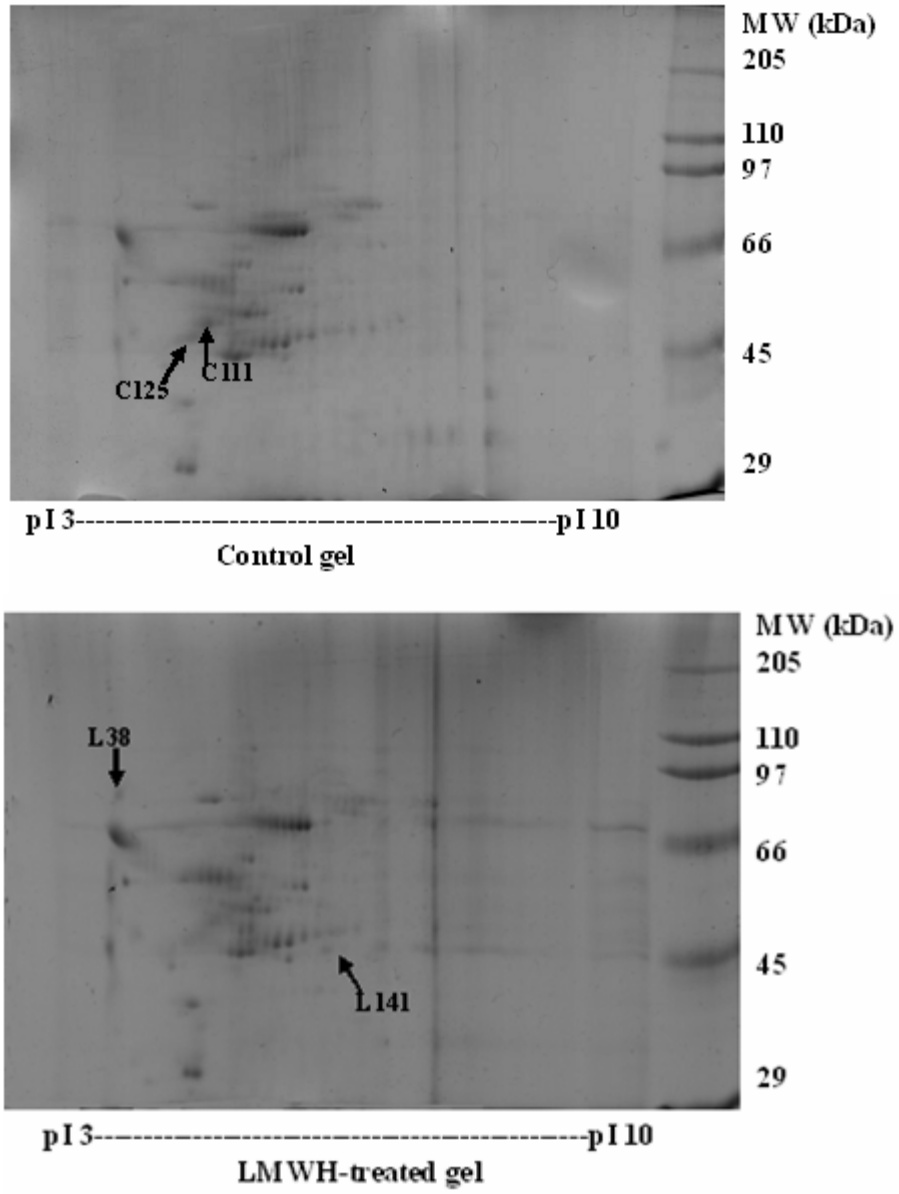

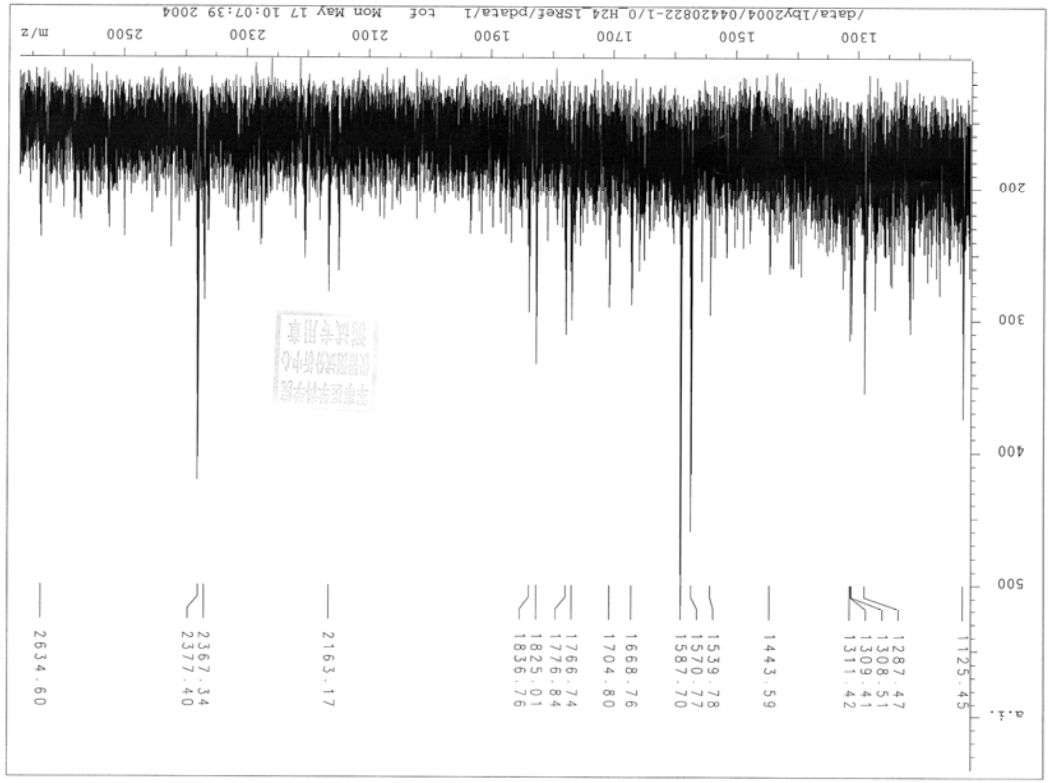

B

JPET Fast Forward. Published on July 6, 2011 as DOI: 10.1124/jpet.111.182055
This article has not been copyedited and formatted. The final version may differ from this version.

C

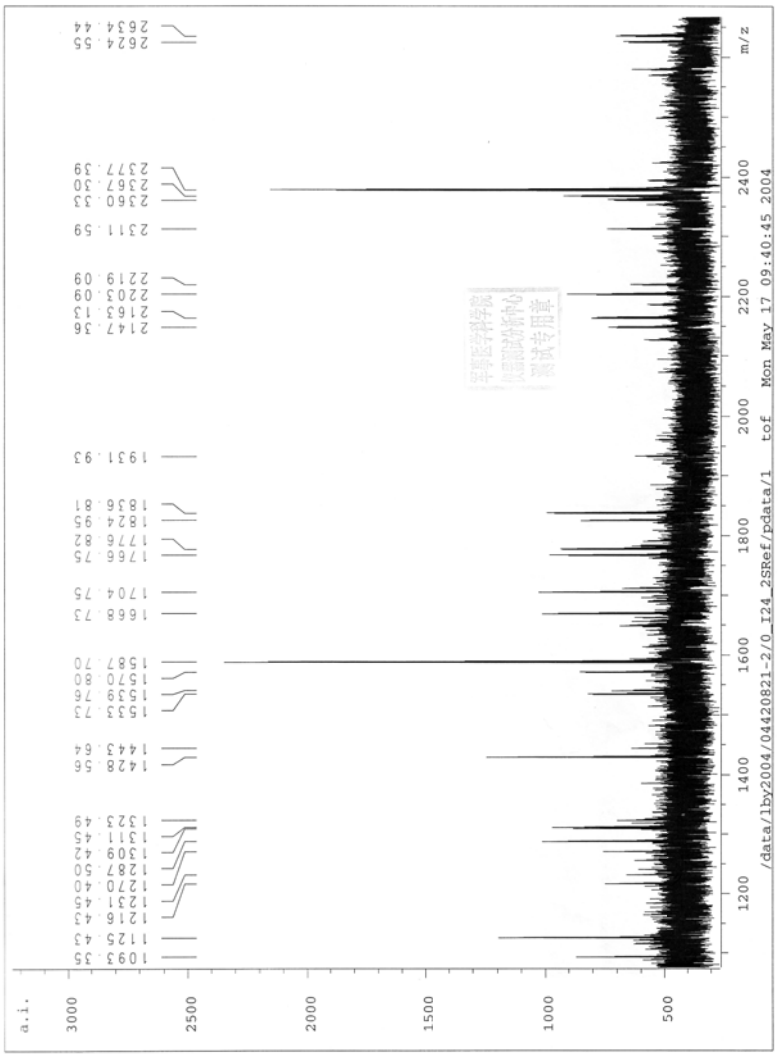

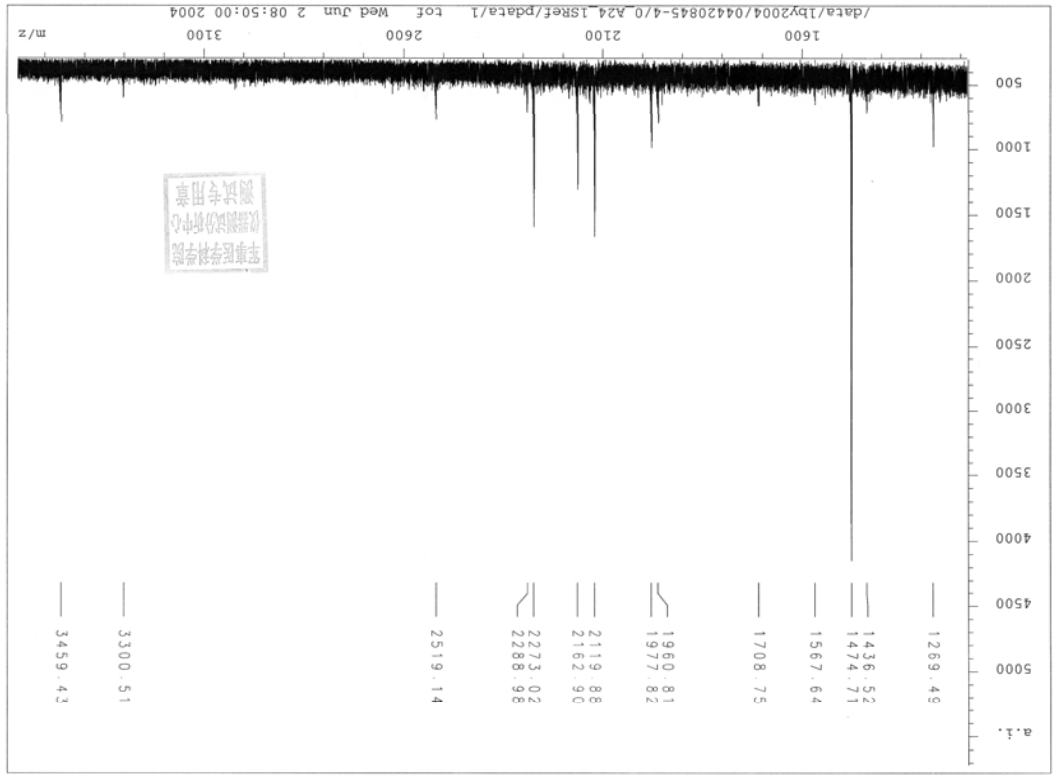

D

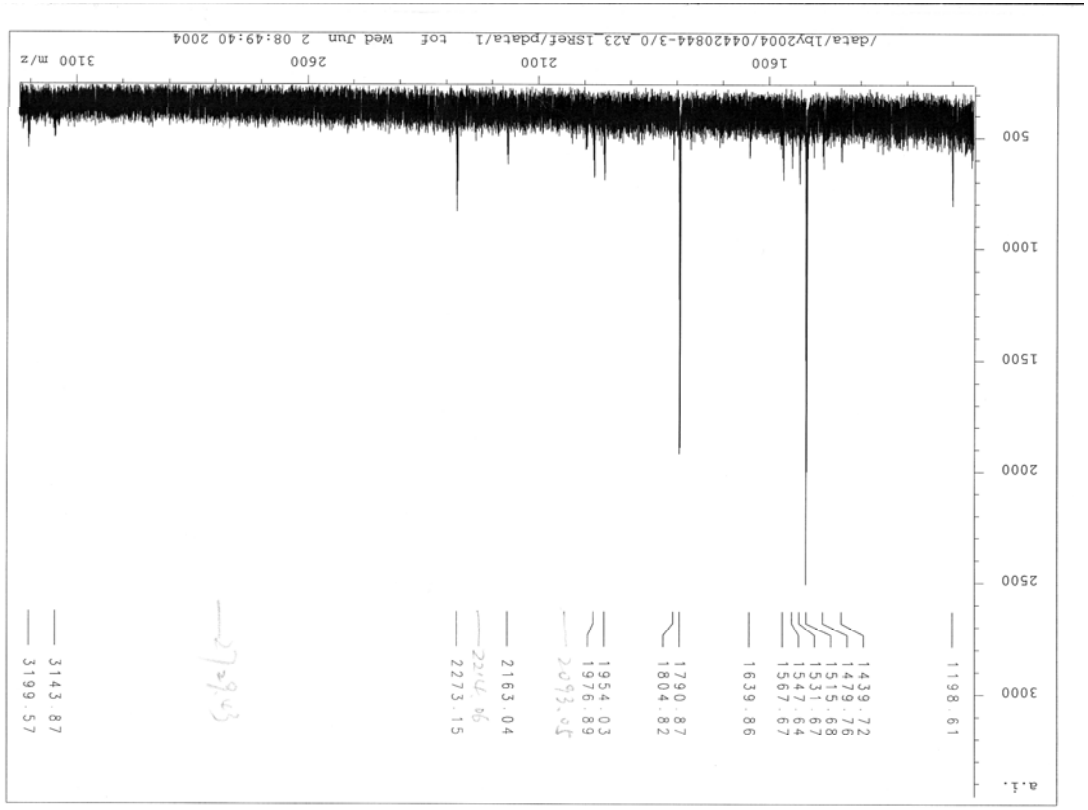

E

JPET Fast Forward. Published on July 6, 2011 as DOI: 10.1124/jpet.111.182055
This article has not been copyedited and formatted. The final version may differ from this version.

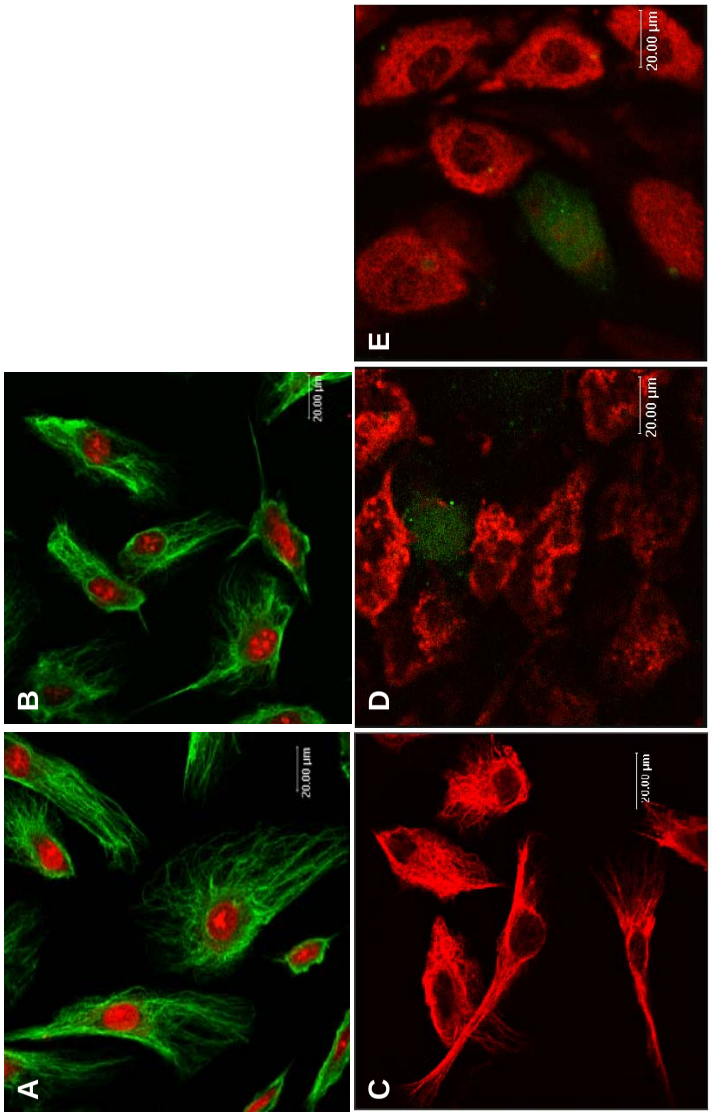

Fig. 6

JPET Fast Forward. Published on July 6, 2011 as DOI: 10.1124/jpet.111.182055
This article has not been copyedited and formatted. The final version may differ from this version.

F

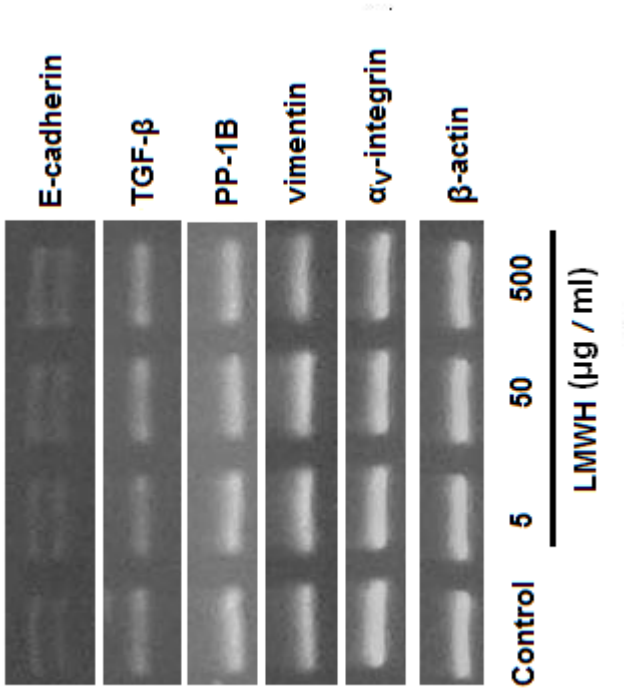

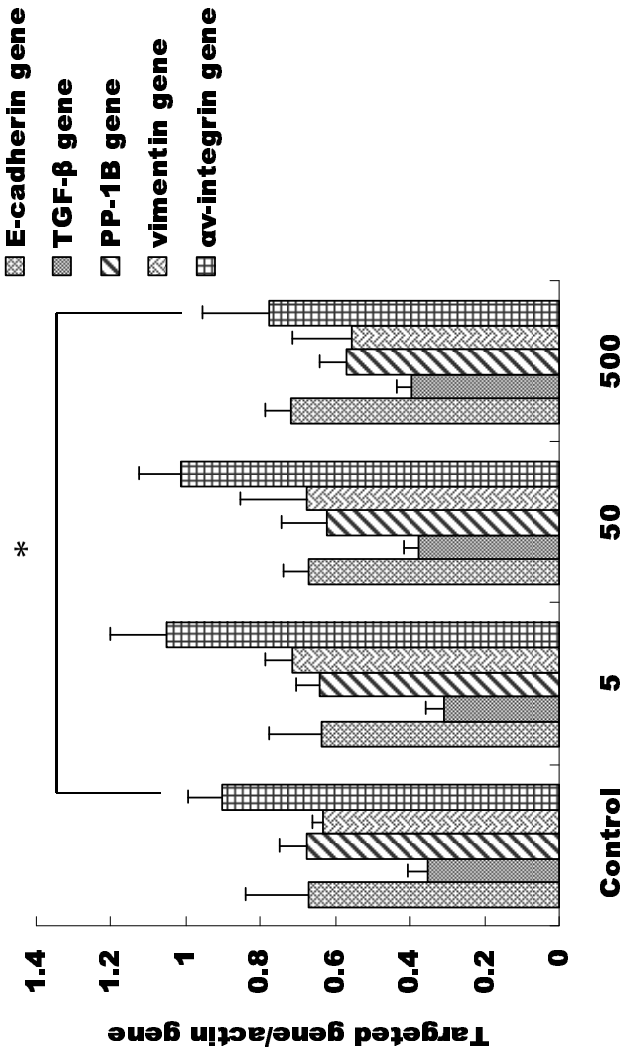

JPET Fast Forward. Published on July 6, 2011 as DOI: 10.1124/jpet.111.182055
This article has not been copyedited and formatted. The final version may differ from this version.

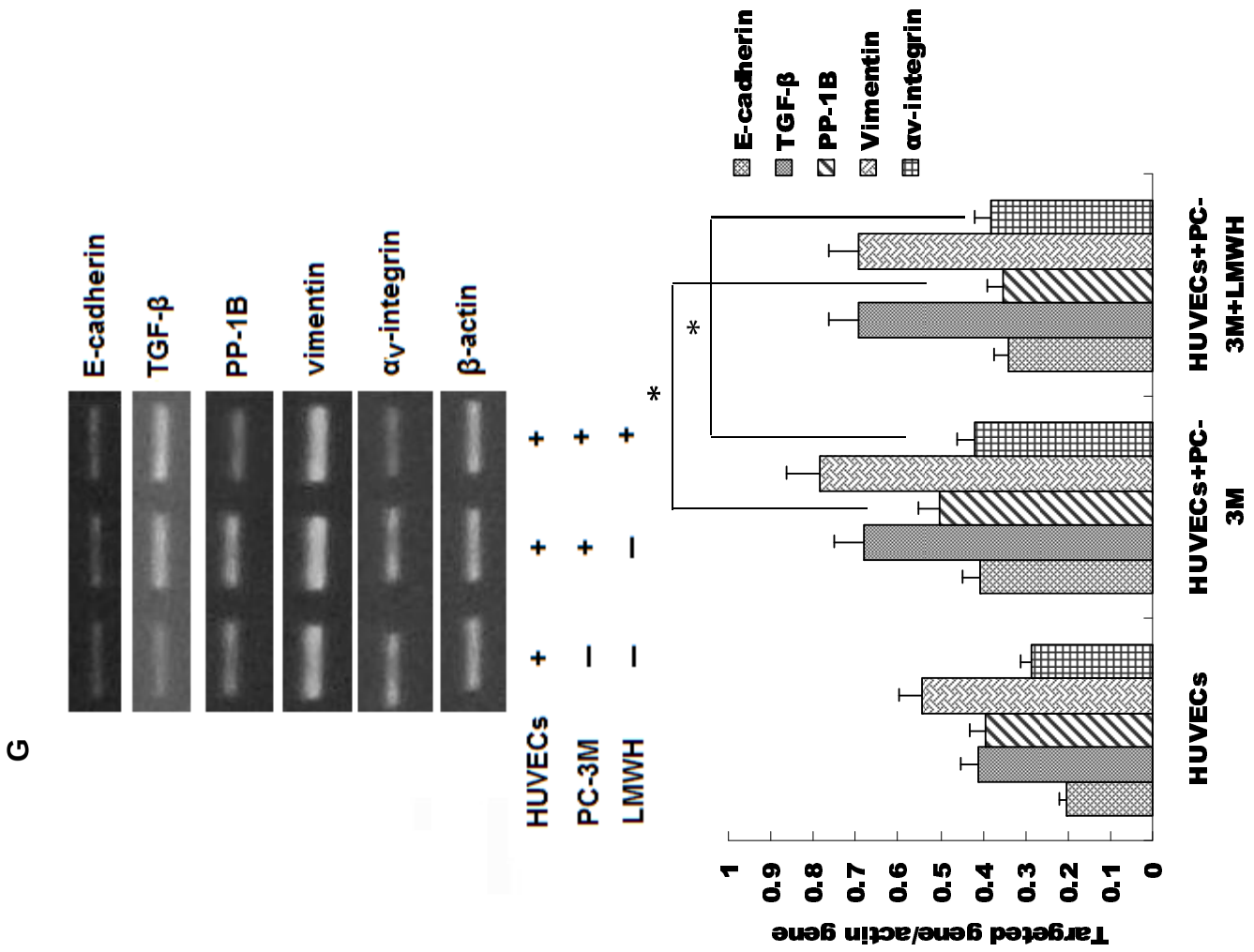

JPET Fast Forward. Published on July 6, 2011 as DOI: 10.1124/jpet.111.182055
This article has not been copyedited and formatted. The final version may differ from this version.

Fig. 7

A.

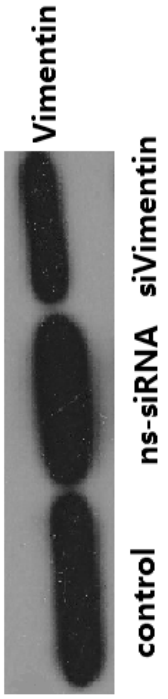

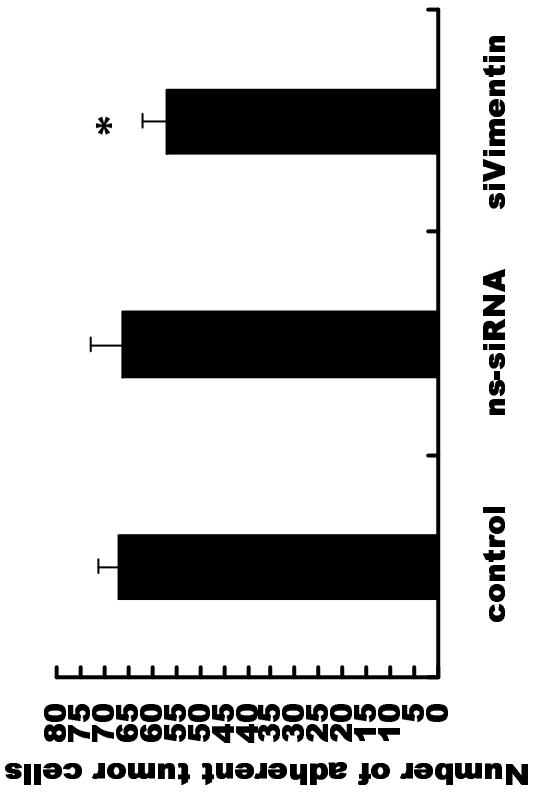

JPET Fast Forward. Published on July 6, 2011 as DOI: 10.1124/jpet.111.182055
This article has not been copyedited and formatted. The final version may differ from this version.

B.

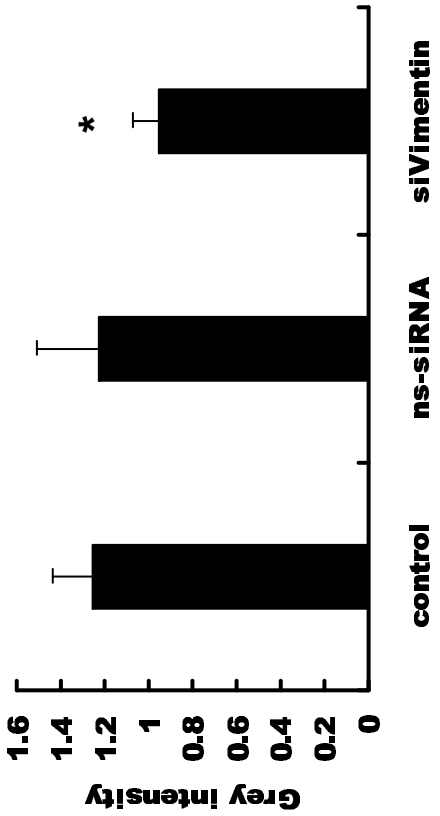

JPET Fast Forward. Published on July 6, 2011 as DOI: 10.1124/jpet.111.182055
This article has not been copyedited and formatted. The final version may differ from this version.

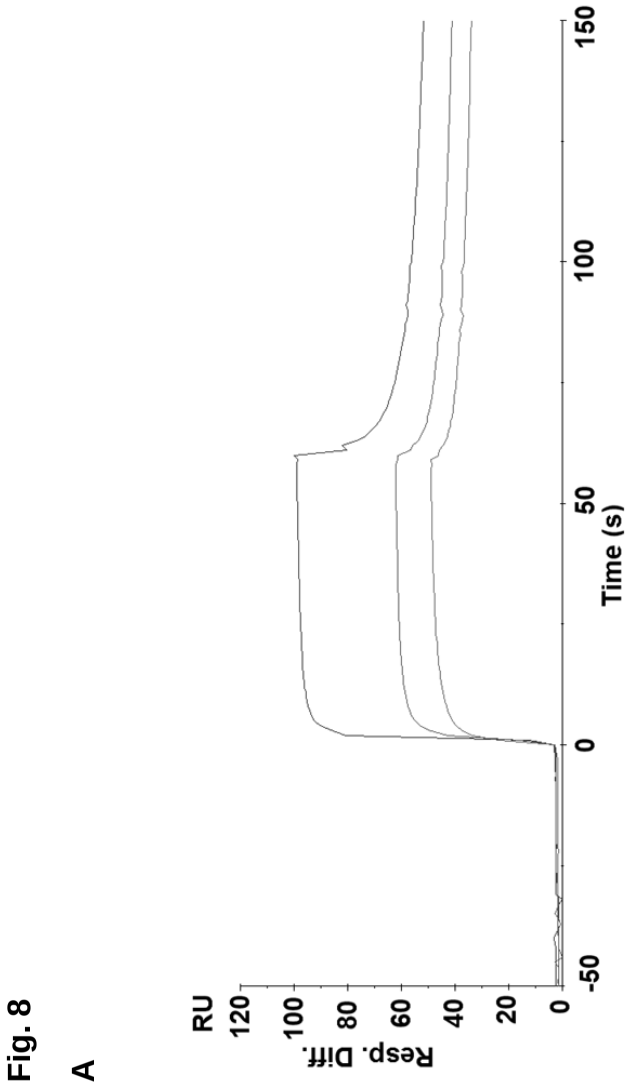

Fig. 8

B